

The W Cell Pathway to Cat Primary Visual Cortex

JOHN C. ANDERSON, NUNO MAÇARICO DA COSTA,* AND KEVAN A.C. MARTIN
Institute for Neuroinformatics, University of Zürich, and ETH Zürich, 8057 Zürich, Switzerland

ABSTRACT

The thalamic input to area 17 in the cat can be divided into at least three parallel pathways, the W, X, and Y. Although the latter two are some of the best studied synaptic connections in the brain, the former remains poorly understood both in structure and in function. By combining light and electron microscopy, we have reconstructed in 3-D single W axons and described quantitatively the synapses that they form. We have also made a structural comparison of reconstructed synapses from the three visual pathways. Thalamic axons were labeled *in vivo* by injections of biotinylated dextran amine into the dLGN. W axons originating from C laminae injections arborized in layers 1, 2/3, and 5. Axons that traversed layer 1 supplied a few descending collaterals to

layer 2/3, but the most extensive innervation in layer 2/3 was provided by axons ascending from the white matter. Most W boutons formed a single synapse, dendritic spines being the most common target, with dendritic shafts forming the remaining targets. In layer 1, the area of the postsynaptic density of spine synapses ($0.16 \mu\text{m}^2$) was significantly larger than that of layers 2/3 ($0.11 \mu\text{m}^2$) and 5 ($0.09 \mu\text{m}^2$). Synapses from X and Y axons in layer 4 were similar in size to synapses formed by W boutons in layer 1. In layer 1, the main targets of the W axons are likely the apical dendrites of pyramidal cells, so that both proximal and distal regions of pyramidal cell dendritic trees can be excited by the W pathway. *J. Comp. Neurol.* 516:20–35, 2009.

© 2009 Wiley-Liss, Inc.

Indexing terms: visual cortex; dLGN; light and electron microscopy; W pathway; X pathway; Y pathway

The axons of the W cells of the dorsal lateral geniculate nucleus (dLGN) of the cat form one of the three major pathways that connect the retina to the visual cortex. W cells are found only in the C laminae of the dLGN (Guillery, 1966; O'Leary, 1940), but their axons provide a widespread innervation of cortical areas 17, 18, 19, 20a, 20b, 21a, PLLS, PMLS, and VLS (Boyd and Matsubara, 1996; Ferster and LeVay, 1978; Geisert, 1980; Hollander and Vanegas, 1977; Kawano, 1998; Laemle, 1975; LeVay and Gilbert, 1976; Leventhal, 1979; Raczkowski and Rosenquist, 1980). In area 17, tracer experiments indicate that W axons innervate layers 1, 2/3, and 5 (Kawano, 1998; LeVay and Gilbert, 1976; Leventhal, 1979), whereas layers 4 and 6 receive input from the X and Y cells of the dLGN.

A bold attempt was made by Ferster and LeVay (1978) to describe the structure of individual thalamic axons at the light microscopic level. They labeled axons by pressure injecting horseradish peroxidase (HRP) into the white matter underlying area 17. These injections labeled many different axons, and so the authors inferred the identity of X, Y, and W dLGN axons based on the layers of termination and the diameter of the axon. Because layer 4 in area 17 was known to be the major target of X and Y axons, the author's inference had a high probability of being correct, and subsequently a direct identification was made by several groups who recorded and labeled X and Y axons by intraxonal injections (Freund et al., 1985a,b; Gilbert and Wiesel, 1979, 1983; Humprey et al., 1985a,b). However, outside layer 4, there are many other

possible sources for the arborizations that Ferster and LeVay (1978) tentatively identified as W. Other thalamic nuclei such as the lateral posterior nucleus (Abramson and Chalupa, 1985; Symonds et al., 1981) and medial interlaminar nucleus (Leventhal, 1979) have projections outside layer 4, as does the claustrum (LeVay and Sherk, 1981) and other cortical areas (Henry et al., 1991; Shatz, 1977). Thus, the morphology of the W axons remains uncertain, and, unlike the case for X and Y axons, we know nothing of their synaptic connections.

The projection of W axons to layer 1 is also significant given our ignorance of the inputs to this layer. At present we do not know the source of 93% of the 19×10^9 asymmetric synapses found in layer 1 (Binzegger et al., 2004) that are likely to be afferents from other cortical and subcortical regions, includ-

Grant sponsor: European Union; Grant number: SECO 216593 (to K.A.C.M.); Grant sponsor: Human Frontier Science Program; Grant number: RG0123/2000-B (to K.A.C.M.); N.M.C. was a fellow from Fundação para a Ciência e Tecnologia in the Gulbenkian PhD Program in Biology and Medicine with grant number SFRH/BD/2724/2000 (to N.M.C.).

*Correspondence to: Nuno Maçarico da Costa, Institute for Neuroinformatics, University of Zürich, and ETH Zürich, Winterthurerstr. 190, 8057 Zürich, Switzerland. E-mail: ndacosta@ini.phys.ethz.ch

Received 22 December 2008; Revised 18 February 2009; Accepted 27 March 2009

DOI 10.1002/cne.22085

Published online April 3, 2009 in Wiley InterScience (www.interscience.wiley.com).

ing the C laminae of the dLGN. Although the W input to layer 1 is not expected to be massive enough to bridge the gap for unassigned synapses in layer 1, it certainly is one of the contributors about which we know very little. The aim of the present study was to study at the light and electron microscopic levels the arborizations of thalamic W neurons in area 17.

MATERIALS AND METHODS

The material used here was taken from seven hemispheres of five adult male cats. The experimental protocols for the project "Microcircuits of neocortex" were approved by the Canton of Zurich Veterinary Office, which issued the licence No. 50/3002 to K.A.C.M. Animals were prepared for surgery after the administration of a subcutaneous premedication of xylazine (Rompun, Beyelar; 0.5 mg/kg)/ketamine (Narketan 10, Vetoquinol AG, CH; 10 mg/kg). Surgery was performed with animals under additional gas anesthesia with 1–2% halothane (Arovet AG, CH) in oxygen/nitrous oxide (50/50%). The femoral vein was cannulated for the delivery of alphaxalone/alphadalone (Saffan; Glaxo) to establish complete balanced anesthesia. Afterward, the cat was intubated and moved to a stereotaxic apparatus, where it was respirated artificially with a mixture of oxygen/nitrous oxide (30/70%), and the end-tidal CO₂ was maintained at 4.5%. EEG, heart rate, end-tidal CO₂, and rectal temperature were monitored continuously.

The classification of the lamina of the dLGN by Guillery (1970) and Hickey and Guillery (1974) was used. They divide the A laminae into A and A1 and the C laminae into C, C1, C2, and C3. Each animal received ionophoretic injections of the neuronal tracer biotinylated dextran amine (BDA; MW 10,000; Molecular Probes, Leiden, Netherlands) into the C and/or the A laminae of the LGN. Each injection site was associated with its cortical termination site by virtue of the precise retinotopic mapping of the dLGN projection to area 17. The correct layer in the dLGN was located with a tungsten recording electrode at appropriate stereotaxic coordinates (Clarke and Henderson, 1914; Sanderson, 1971). Eye movements were reduced by a low dose of the muscle relaxant gallamine triethiodide given intravenously (12 mg induction dose, 5 mg/kg⁻¹/hr⁻¹ thereafter; Sigma Aldrich, Switzerland). When the appropriate lamina and location of the dLGN was found, the depth was noted and the tungsten electrode was replaced by a BDA-filled glass micropipette, and the recordings were repeated.

Ionophoretic injections were made for 15–20 minutes at 2–4 μ A. The BDA was delivered as a 10% solution in 0.01 M phosphate buffer, pH 7.4 (PB), plus 0.2 M KCl or 0.05 M Tris plus 0.4 M KCl. Delivery of the muscle relaxant was stopped 2–3 hours before the end of the surgery. Respiration and muscular tonus were monitored to assess the animal's recovery. After a 5–11-day survival period, anesthesia was again induced with ketamine/xylazine and the cats were deeply anaesthetized with i.v. Saffan (20 mg/kg). The cats were perfused transcardially with a normal saline solution, followed by a solution of 4% paraformaldehyde, 0.3% glutaraldehyde, and 15% picric acid in 0.1 M PB, pH 7.4. The brain was blocked in stereotaxic planes, and the block was sunk in a series of sucrose solutions of 10%, 20%, and 30% in 0.1 M PB to serve as cryoprotectant. The blocks were then freeze-thawed in liquid nitrogen and washed in 0.1 M PB for at least 1 hour. Sections were cut in the coronal plane on a Vibratome at 80

μ m thickness and collected in 0.1 M PB. After washes in TBS, the sections were left overnight (5°C) in an avidin-biotin complex (ABC Elite Kit; Vector Laboratories, Burlingame, CA). The peroxidase activity was identified by using 3,3-diaminobenzidine tetrahydrochloride (Sigma-Aldrich, Germany) with nickel intensification. After assessment by light microscopy (LM), selected regions of tissue were treated with 1% osmium tetroxide in 0.1 M PB. Dehydration through alcohols (1% uranyl acetate in the 70% alcohol) and propylene oxide allowed flat mounting in Durcupan (Fluka Chemie, Switzerland) on glass slides.

Light microscopic observations of labeled axons were carried out to locate and select regions of interest for electron microscopy (EM). We reconstructed individual collaterals where possible (using TRAKA, an in-house LM-digitization package), although correlated light and electron microscopy was not possible because of the density of labeled collaterals. Serial ultrathin sections were collected at 60 nm thickness on Pioloform-coated single slot copper grids. Labeled boutons were photographed at a magnification of $\times 21,000$. Synapses and associated structures were classified by conventional criteria. Serial sections were digitized and reconstructed in Trakem, an in-house EM-digitization package, or Reconstruct (Fiala, 2005). To measure and display the postsynaptic densities (PSDs) of labeled boutons, we used software developed by ourselves, which has been described elsewhere (see Materials and Methods in Anderson et al., 1998). We also measured the cross-sectional area of the presynaptic bouton associated with the longest PSD of each synapse in a single section (see Materials and Methods in Ahmed et al., 1994). Synapses formed by unlabeled boutons in the neuropil surrounding the W boutons were selected by using the physical disector method (Sterio, 1984), and their postsynaptic targets were identified by standard ultrastructural criteria (Peters et al., 1991). Adobe Photoshop CS4 was used for histogram equalization and contrast enhancement in digital photomicrographs. Adobe Illustrator CS4 was used to prepare the figures.

RESULTS

Light microscopy observations

Injections in the C laminae. In total, 11 injections were made in the C laminae in four cats. The ionophoretic injections of BDA into the C laminae of the LGN were clearly visible in the light microscope after the histological processing (Fig. 1). The injection sites were small ($\sim 300 \mu$ m) and usually restricted to the C laminae, with the exception of two injections where there was some spread of the tracer into the overlying lamina A1. Cells at the injection site were well labeled, and their axons left the dLGN and entered the optic radiations. In the cortex, labeled axons were seen in areas 17, 18, 19, and 20, but only the axons projecting to area 17 will be considered here. The termination sites in area 17 also tended to be small, with the labeled axons arising from a relatively small (~ 1 mm diameter) patch of white matter, but in layer 1 the labeled axons extended laterally as much as 5 mm. Within the white matter, the labeling was seen mostly at the cut ends, which is evidence that the axons were myelinated, because the avidin-HRP was not able to penetrate the myelin sheath. Labeled axons arose from the white matter to pass radially through the cortical laminae and branched to form collaterals in layers 5,

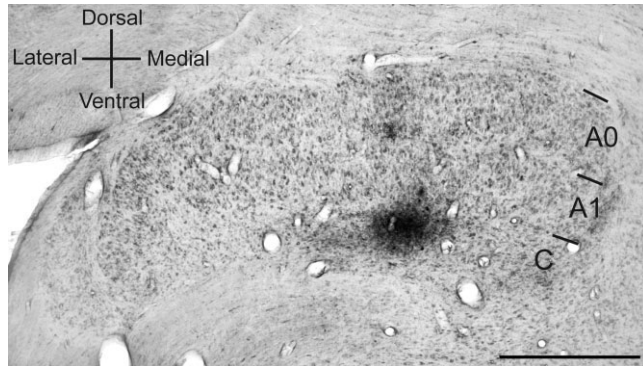


Figure 1. Location of injection site. Photomicrograph of coronal section through the dorsal lateral geniculate nucleus of the cat (dLGN) counterstained with neutral red. This section shows an example of a BDA injection site located in lamina C. Laminae are indicated to the right. Scale bar = 1 mm.

2/3, and 1 (Fig. 2). Two of the injections were centered on the upper part of the C laminae and produced labeled terminals in layer 4 and 2/3 but very little in layer 1. In addition, when only the dorsal C laminae were injected, there was much less label in layer 2/3, and most of the axons labeled were of the type shown in Figure 3. Axons were of small caliber (diameter $<1 \mu\text{m}$) and proved difficult to follow with the light microscope. We saw no retrograde labeling.

In layer 1, single axons traversed just below the surface of the cortex for distances up to 4 mm. Numerous en passant varicosities formed along unmyelinated portions of the axon. These long axons emitted fine collaterals, most of which remained in layer 1, but some occasionally descended into layer 2/3 (Fig. 3A,B). Subsequent EM showed that the varicosities on axons with intermittent myelination in layer 1 were usually nonsynaptic and contained mitochondria, but similar bouton-like varicosities on unmyelinated collaterals always formed synapses. Both long ($>100 \mu\text{m}$) and short ($\sim 10\text{--}20 \mu\text{m}$) unmyelinated, bouton-bearing collaterals projected through layer 1. Most of the axons in layer 1 could not be traced from the white matter or even beyond the layer 3/4 border (Fig. 3A,B). Among those layer 1-projecting axons that could be traced from the deep cortical layers (Fig. 3C,D), the arborization in the upper layers appeared to be less extensive in layer 1 than in layer 2/3. The true extent of the projection in layer 1 of these axons was always limited by visibility. Axons close to the pial surface were traced with great difficulty because of the abrupt changes in luminance between the osmicated section and the mounting medium. Most of the axons in layer 1 traversed through the upper part of the layer as also observed in the axons described by Ferster and LeVay (1978). Axons that produced collaterals in layer 5 also could be traced to layer 1.

Layers 2 and 3 were richly innervated by collaterals that branched in layer 3 and sent fine, bouton-covered axon branches up through layer 2 (Figs. 4, 5) and occasionally into layer 1 (Fig. 4B). These axons also formed collaterals in layer 5. The coverage area in layer 2/3 of the three axons illustrated in Figures 4A,B and 5 was 0.23 mm^2 , 0.11 mm^2 , and 0.95 mm^2 , respectively.

Although all axons that we traced from the white matter had collaterals in layer 5, these collaterals were extremely fine and difficult to follow, an onerous task relieved only by rare encounters with thicker axons. The fine collaterals passed back and forth between lamina boundaries, branching frequently and sometimes showing a recurrent pattern of innervation. Boutons throughout tended to be small, almost dust-like swellings ($\sim 0.5 \mu\text{m}$) mostly of the en passant variety. Those of layer 5 tended to be the smallest and those of layer 1 the largest.

Injections in the A lamina. Two hemispheres from two cats were used for the A laminae study. Ten ionophoretic injections of BDA into the A laminae of the dLGN were clearly visible in the light microscope. Eight of the injections were restricted to the contralateral A lamina, in the other two, the injection site included the A and A₁ laminae. In area 17, they formed clusters of axons and boutons in layers 4 and 6.

Electron microscopy

Terminals originating from the C laminae. We sampled a total of 231 synaptic boutons from layers 1, 2/3, and 5 (95 from layer 1, 69 from layer 2/3, and 67 from layer 5) in two cats. Almost half (118 boutons) were sectioned serially and completely reconstructed. The remainder (113) were less complete, often single sections, but more if it was necessary to the identification of the postsynaptic target. Together these sections provided 260 labeled synapses all of which were asymmetric (Gray's type 1).

The reaction end product was dark and varied in intensity between boutons and within boutons. Vesicles and mitochondria were clearly visible inside the boutons, and the synaptic clefts were not obscured by label. The cut ends of myelinated fibers were darkly labeled, but myelinated axons were weakly labeled. Most synaptic boutons were small ($\sim 0.5 \mu\text{m}$ diameter), compact structures, containing one or two mitochondria and a cluster of vesicles at the region of the synaptic specialization (see, e.g., Figs. 6, 7).

Synapses formed with spines. We used standard ultrastructural criteria to classify targets (Peters et al., 1991), although in cases of complete bouton reconstructions there was no doubt about the identity of the synaptic targets. Small spines were the most frequent targets of labeled boutons. Sometimes a spine neck could be found emerging from these small spine heads (Fig. 6A), but only rarely could a neck be followed back to the parent dendrite. Nine of the target spines ($\sim 4\%$ of total) formed a second, symmetric synapse with an unlabeled bouton. Two such dual-input spines were found in layer 1, two in layer 2/3, and five in layer 5. We found spine synapses in 84 of 98 cases in layer 1, 78 of 82 cases in layer 2/3, and 66 of 80 cases in layer 5. The remaining synapses were formed with dendritic shafts. Figure 7B shows a labeled bouton from layer 2/3 that formed a synapse with a small, bud-like process or gemmule. The gemmule-bearing dendrite followed a tortuous path and formed no other synapses over several micrometers of reconstructed profile. No other spines or gemmules were seen on the dendrite. The gemmule contained a spine apparatus and contained no microtubules; we classified it as a spine.

Synapses formed with dendritic shafts. Dendritic shafts were also targets of labeled boutons ($\sim 14\%$ of all labeled boutons). Serial reconstructions helped greatly in deciding

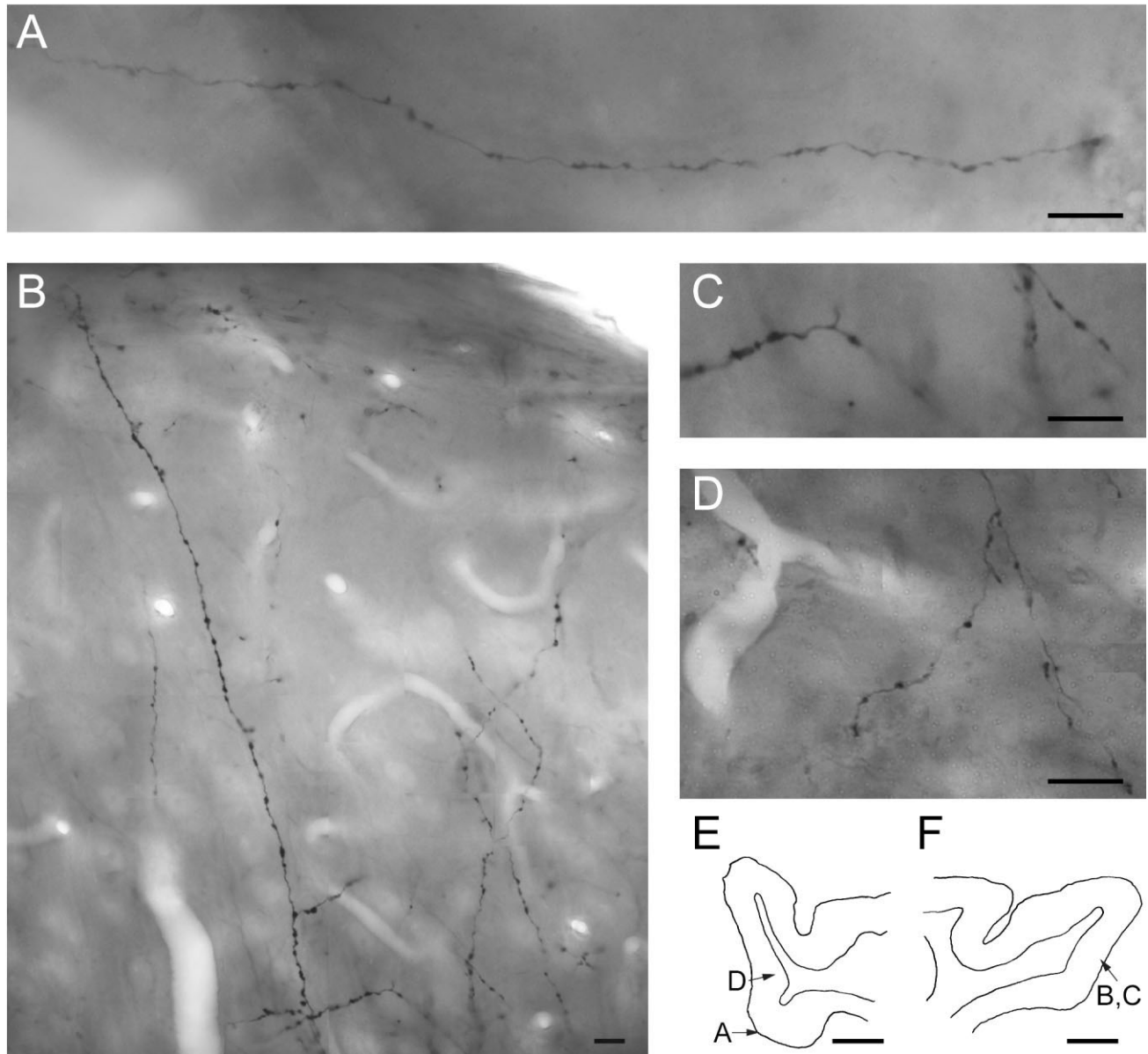


Figure 2. Photomontages of light micrographs of W axons in layer 1 (A), layer 2/3 (B,C), and layer 5 (D). C is a higher magnification of B. E,F: Schematic of coronal sections through area 17, with arrows indicating the location of the axons shown in A–D. Scale bars = 10 μm in A–D; 2 mm in E,F.

that different types of dendritic shafts were targets. Some target dendritic shafts contained few mitochondria, and they seldom formed additional synapses on the shaft (Fig. 7C, but see also Fig. 7B). These features are characteristic of spiny neurons.

When reconstructed over several serial sections, smooth dendrites (Ahmed et al., 1997; Kisvarday et al., 1985; Peters and Saint Marie, 1984; Somogyi et al., 1983) formed synapses with other unidentified boutons, contained numerous mitochondria, bore no spines, and had variable diameter (Figs. 6D, 7A). In layer 1, 8 of 14 synapses formed with dendritic shafts were on smooth (putative GABAergic) neurons, in layer 2/3 1 of 4, and in layer 5 8 of 10.

Synapses formed with the cell body. Only one cell body, located in layer 5, formed synapses with labeled boutons. The four labeled boutons were small (~ 500 nm in diameter by ~ 200 nm thickness), and the cell body also received synapses from unidentified boutons, both symmetric and asymmetric. The soma was filled with cytoplasmic organelles and rough endoplasmic reticulum. These features indicate that the cell body was that of a smooth neuron.

Reconstruction of postsynaptic densities. Serially reconstructed W boutons allowed us to see the full extent of the postsynaptic densities, these are presented as 2-D en face projections in Figure 8. The dark reaction end product inside the bouton tended to obscure the presynaptic mem-

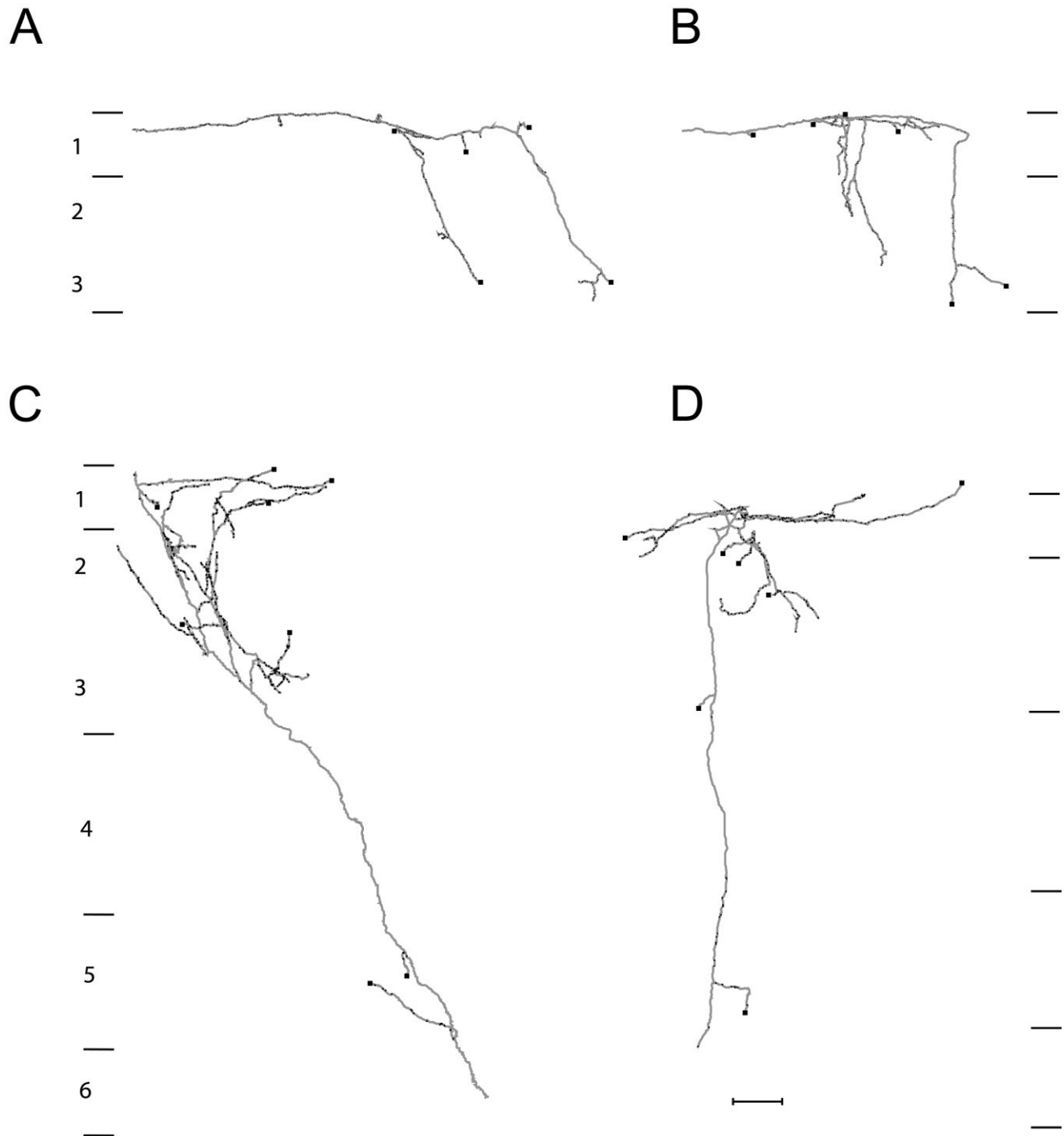


Figure 3. Light microscopic reconstructions of four W cell axons (gray) with boutons (black). **A,B:** Axons passing through layer 1 that could not be followed back to white matter and showing collaterals descending into layer 2/3 (axon in A had 285 reconstructed boutons; axon in B had 186 reconstructed boutons). **C,D:** Axons arising from deep layers and arborizing in layers 1 and 2/3 (axon in C had reconstructed 379 boutons, axon in D had reconstructed 265 boutons). The reconstructions are of incomplete axons; black squares denote the end of incomplete axon collaterals. Lamina boundaries are indicated. Scale bar = 100 μm .

brane. However, the postsynaptic specialization was not affected by the labeling and was relatively easy to reconstruct. We have used this technique previously to visualize postsynaptic densities (Anderson et al., 1998; Anderson

and Martin, 2002, 2005, 2006) in the monkey visual cortex. The postsynaptic density can be perforated and, as in previous work, such perforated synapses were mostly observed for spines. We also observed thalamic axons form-

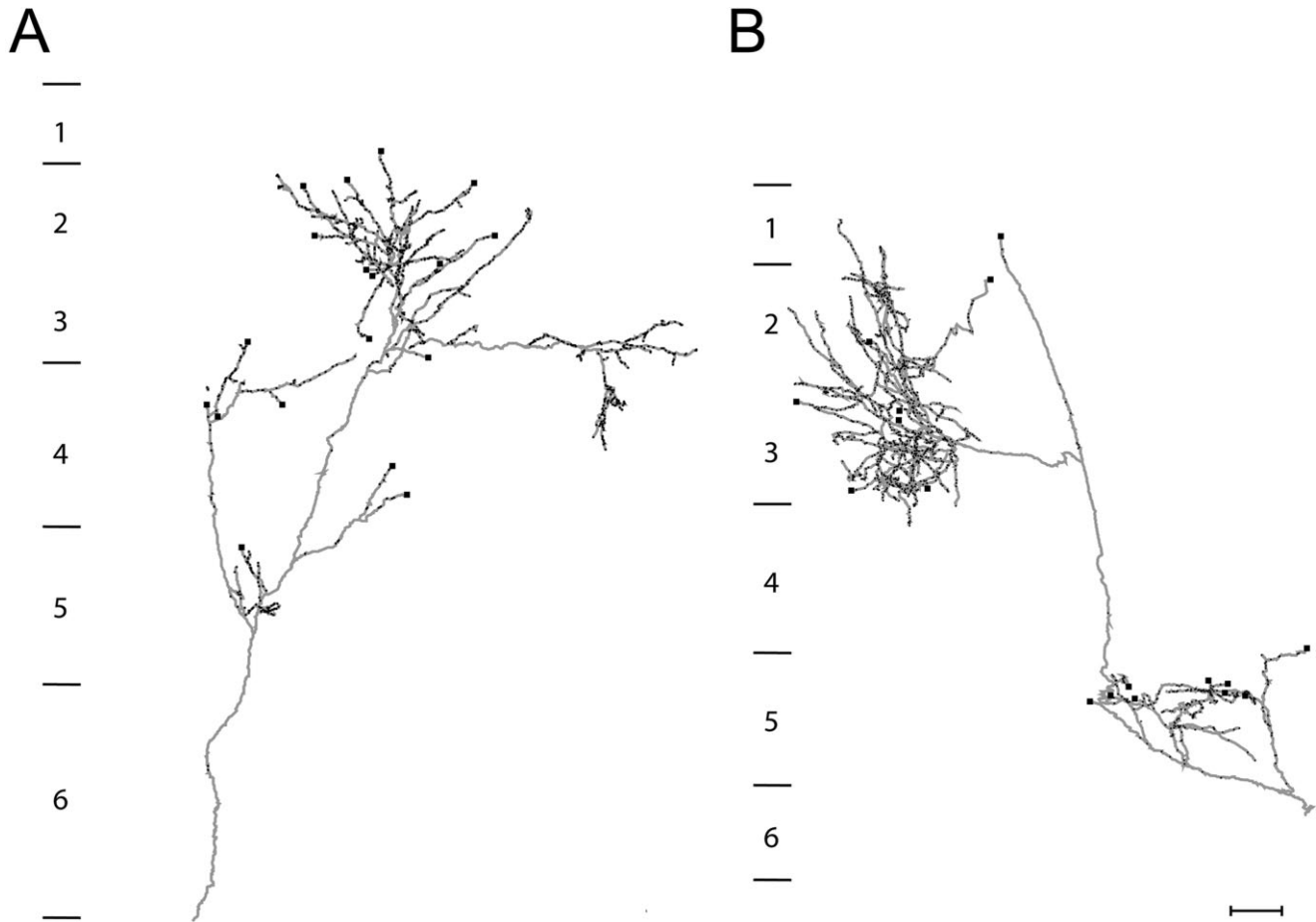


Figure 4. Light microscopic reconstructions of two W cell axons (gray) with boutons (black). **A,B:** Axons arising from white matter and arborizing principally in layers 2 and 3 (axon in A had 951 reconstructed boutons; axon in B had 1391 reconstructed boutons). The reconstructions are of incomplete axons; black squares denote the end of incomplete axon collaterals. Laminae boundaries are indicated. Scale bar = 100 μm .

ing large synapses with dendritic shafts, and these were also perforated (Figs. 8, 9). The simpler disc shape was usually associated with small synapses.

There were differences in the distributions of synapse areas formed with spines and dendrites between the laminae (Fig. 10). In layer 1, the spine synapses were significantly larger than dendritic shaft synapses ($P = 0.0048$, two-tailed t -test); spine synapses had a mean of $0.16 \mu\text{m}^2$ (SEM 0.015, $n = 37$) and dendritic shaft synapses $0.08 \mu\text{m}^2$ (SEM 0.008, $n = 6$). In layers 5, there was no significant difference between synapses formed with spines and dendritic shafts ($P = 0.95$, Kolmogorov-Smirnov test). Spine synapses formed by W boutons had a mean area of $0.09 \mu\text{m}^2$ (SEM 0.01, $n = 33$), whereas those on dendrites had a mean area of $0.16 \mu\text{m}^2$ (SEM 0.07, $n = 8$). Both spine and dendritic synapses in layers 2 and 3 had a mean area of $0.11 \mu\text{m}^2$ (SEM 0.01, $n = 45$ for spines, only two values for dendrite).

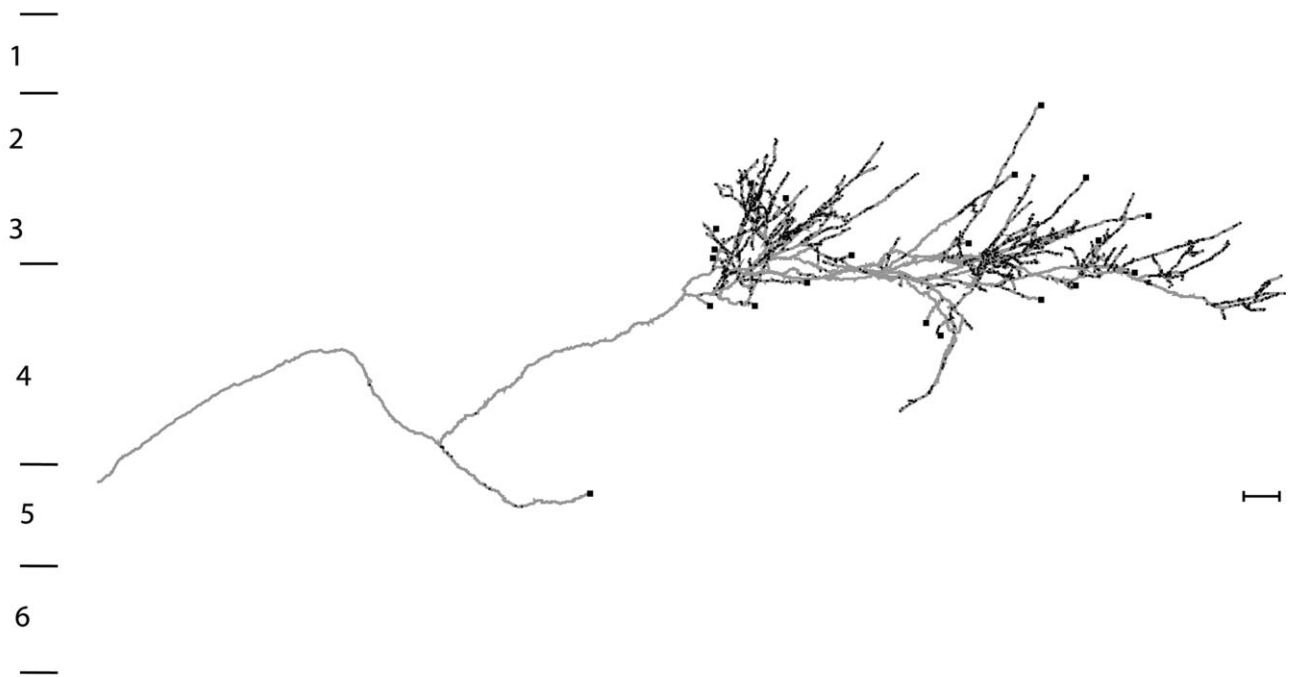
Spine synapses of layer 1 were significantly larger in area than those of layer 5 ($P = 0.0005$, Kolmogorov-Smirnov test) or those of layer 2/3 ($P = 0.009$, Kolmogorov-Smirnov test). The spines synapses of layers 2, 3, and 5 were not significantly different from each other ($P = 0.51$, Kolmogorov-

Smirnov test). The pooled data from all layers of all synapses showed no significant difference between spine and dendrite synapse areas (both means $0.12 \mu\text{m}^2$; $P = 0.21$, Kolmogorov-Smirnov test).

We also reconstructed 86 PSDs from labeled boutons of X and Y axons in layer 4 after injections of the A lamina of the dLGN from two cats. Figure 9 shows the 2-D projections of the layer 4 PSDs. Synapses formed with spines had a mean area of $0.160 \mu\text{m}^2$ (SEM 0.008, $n = 71$), which was smaller than the mean area of the synapses formed with dendritic shafts ($0.273 \mu\text{m}^2$, SEM 0.038, $n = 14$). These two samples were significantly different ($P = 0.005$, Kolmogorov-Smirnov test). The area of the synapses formed by X/Y axons on spines in layer 4 was not significantly different from the area of the synapses formed by W axons in layer 1 ($P = 0.63$, t -test) but was significantly larger than the area of synapses formed in layer 2/3 and 5 ($P = 0.00004$ and $P = 0.000004$, Kolmogorov-Smirnov test).

Figure 11 shows a complete reconstruction of the boutons and target spines that formed the smaller and larger PSD in each layer. Such reconstructions indicated that bouton size might not be related to the area of the synapse. To investigate

A



B



Figure 5. Light microscopic reconstruction of a single W cell axon (gray) with boutons (black). **A:** Axon arising from deep layers and arborizing extensively in layer 2 and 3 (axon had 2,179 reconstructed boutons). **B:** Axon in A rotated and seen from above. The reconstructions are of an incomplete axon; black squares denote the end of incomplete axon collaterals. Lamina boundaries are indicated. Scale bar = 100 μm .

this, we measured the cross-sectional area of the thalamic boutons.

Bouton area. The section containing the longest synaptic profile was selected to measure the cross-sectional area (see Materials and Methods) of 41 boutons in layer 1 (0.33 ± 0.03 ,

mean \pm SEM), 50 boutons in layer 2/3 (0.41 ± 0.03), and 41 boutons in layer 5 (0.23 ± 0.02). In both cats examined, the boutons from layer 5 had cross-sectional areas that were significantly smaller than those of boutons in layer 1 ($P = 0.0123$, Kolmogorov-Smirnov test). Boutons sampled in layer

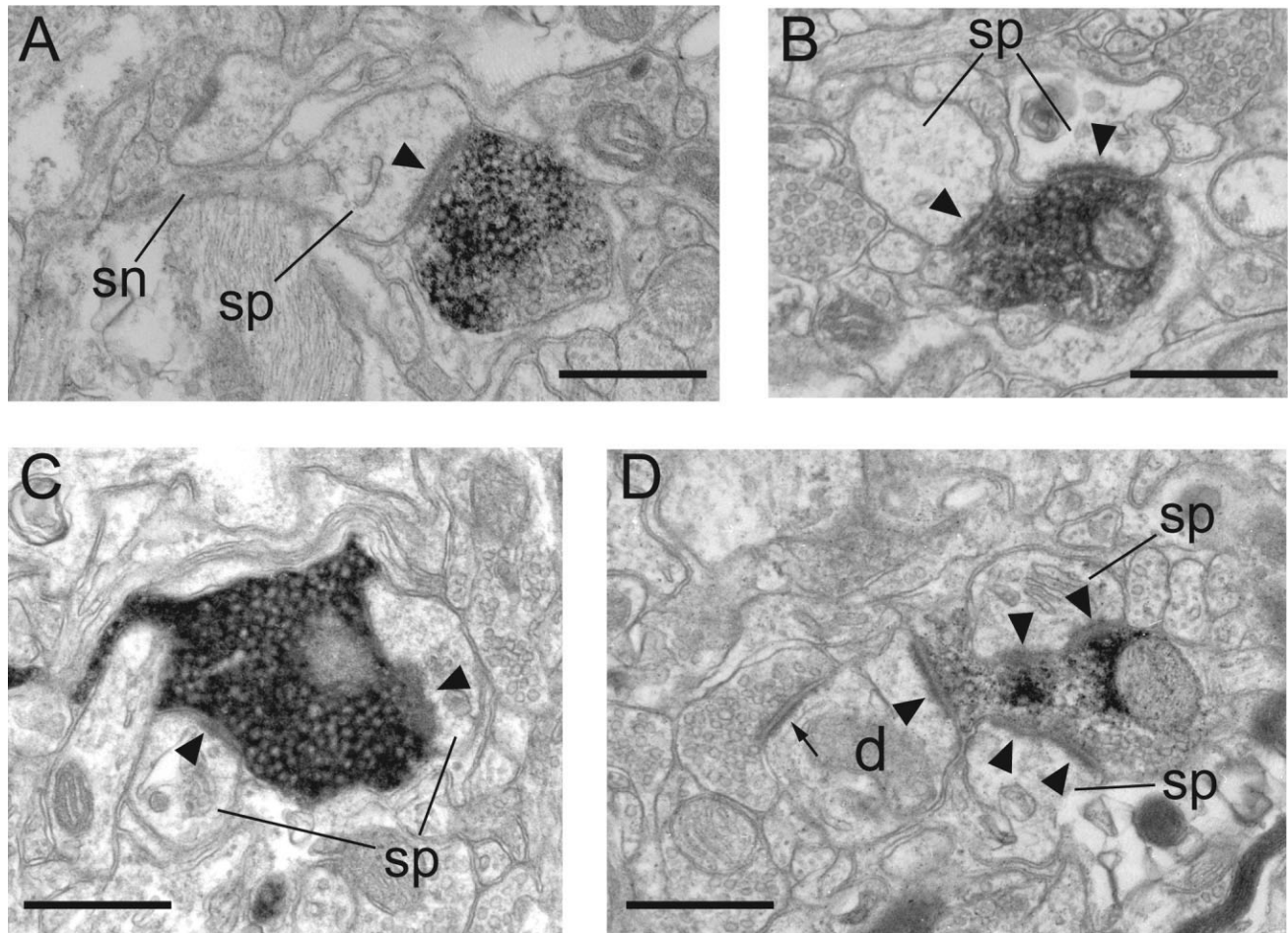


Figure 6.

Electron micrographs of BDA-labeled, electron-dense boutons located in area 17. Examples of synapses formed with the most frequent synaptic target, spines (A–C) and a dendrite (D). A: A bouton in layer 1 forms an asymmetric synapse (arrowhead) with a spine (sp). The spine neck (sn) can be seen attached to the spine. B: Two spines (sp) form asymmetric synapses (arrowheads) with a labeled bouton in layer 1. C: Two spines (sp) form asymmetric synapses (arrowheads) with a labeled bouton in layer 2/3. D: A labeled bouton in layer 5 forms three asymmetric synapses (arrowheads) with two spines (sp) and a dendritic shaft (d). The dendrite forms a second asymmetric synapse (small arrow) with an unidentified bouton. Dendrites such as these containing numerous mitochondria and forming many synapses are characteristic of putative GABAergic neurons. Scale bars = 0.5 μm .

2/3 showed variations in size that were significantly different between animals. One animal had cross-sectional areas comparable to those of layer 1 boutons ($P = 0.6442$, Kolmogorov-Smirnov test), whereas the W boutons of the other cat had larger cross-sectional areas in layer 2/3 ($P = 0.0044$, Kolmogorov-Smirnov test). Between layers, there was no correlation between mean synaptic size and bouton cross-section, so we examined whether this was also the case within a layer. We found that there was very little or no linear correlation between the PSD size of a synapse and the cross-sectional area of the bouton that forms that synapse (layer 1 $r^2 = 0.11$, layer 2/3 $r^2 = 0.0003$, layer 5 $r^2 = 0.2$).

As in layers 2 and 3, even though the area of the synapses in layer 4 was not different in the two cats examined, the cross-sectional area of the synaptic boutons was significantly different between animals (0.873 μm^2 , SEM 0.06, and 0.466 μm^2 , SEM 0.03; $P < 0.01$ 8.2E-8).

Target types. Spines were the dominant synaptic targets of W cell boutons in all layers (Fig. 12A). In layer 1, 86% of

synapses were formed with spines and 14% with dendritic shafts. In layer 2/3, spines accounted for 94% and dendritic shafts 6%. In layer 5, 83% of synapses were formed with spines, 12% with dendritic shafts, and 5% with somata. More than half of the dendritic shaft synapses were formed with dendrites of smooth, putative γ -aminobutyric acid (GABA)-ergic neurons. In the neuropil surrounding the W boutons, 71% of synaptic targets in layer 1 were spines and 29% were dendritic shafts. In layers 2 and 3, 85% of synaptic targets were spines and the remainder dendritic shafts. In layer 5, 77% of synapses were formed with spines and 23% with dendritic shafts. The majority of synapses on dendritic shafts were formed with the dendrites of putative smooth GABAergic neurons. By using a G-test of independence, the proportion of synapses formed with dendritic shafts and spines is independent of the bouton being labeled or not (at a threshold of $\alpha = 5\%$, for all the three layers). We conclude that there is no target specificity of the W boutons with regard to dendritic spines or shafts.

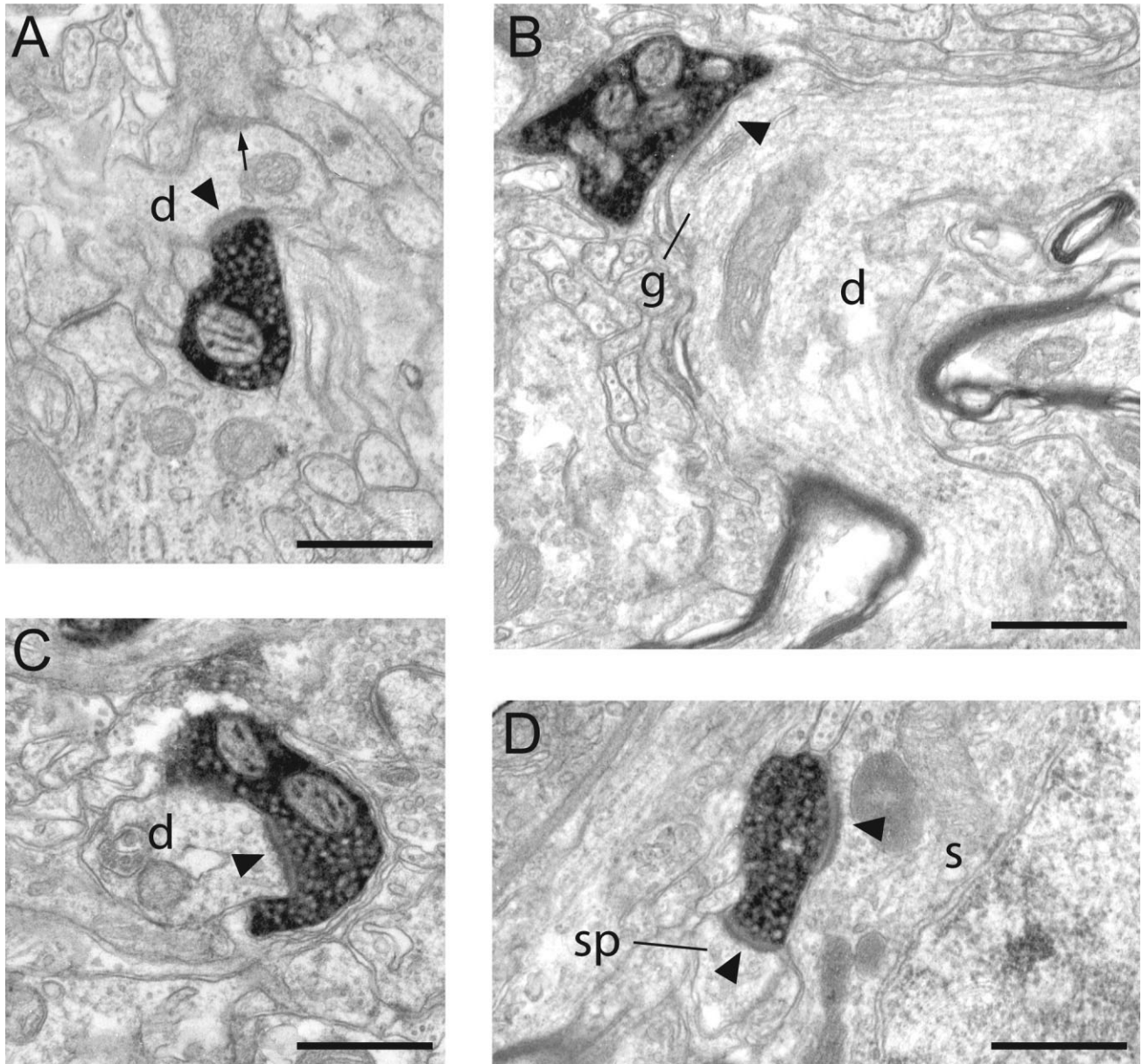


Figure 7.

Electron micrographs of BDA-labeled, electron-dense boutons located in area 17 and forming asymmetric synapses with targets other than spines. **A:** A labeled bouton in layer 1 forms an asymmetric synapse (arrowhead) with a dendritic shaft (d). The dendrite also forms an asymmetric synapse (small arrow) with an unidentified bouton. Partial reconstruction from serial sections showed that the dendrite had a beaded morphology, formed many synapses, and contained numerous mitochondria. These features are characteristic of GABAergic neurons. **B:** A labeled bouton in layer 2/3 forms an asymmetric synapse (arrowhead) with a small bud-like process or gemule (g) containing spine apparatus. The gemule is formed on a large-caliber dendritic shaft (d) that contains few mitochondria and forms synapses infrequently. These features are characteristic of neurons with spiny dendrites. **C:** A small-caliber dendritic shaft (d) in layer 2/3 forms an asymmetric synapse with a dendritic shaft (d). The dendrite forms few synapses and contains few mitochondria. These are features indicative of a spiny neuron. **D:** In layer 5, a labeled bouton forms two asymmetric synapses (arrowheads), with a spine (sp) and a soma (s). Scale bars = 0.5 μm .

It should be noted that, by choosing a labeled bouton, we necessarily bias our sample of synapses from the neuropil. Only random sampling will provide an unbiased percentage of synaptic targets for these layers, as is the case for the study of Beaulieu and Colonnier (1985), who provide an estimate of the proportion of synapses formed with spines, dendrites, and somata for all layers of cat area 17.

Most reconstructed boutons formed only one synapse (Fig. 12A). Occasionally, a single bouton formed a second synapse with a second target and, rarely (three times), with a third. We saw no labeled multiple synaptic inputs to single targets except in the case of a somata in layer 5, which formed synapses with four labeled boutons. However, because only portions of single dendrites were reconstructed, we cannot determine the

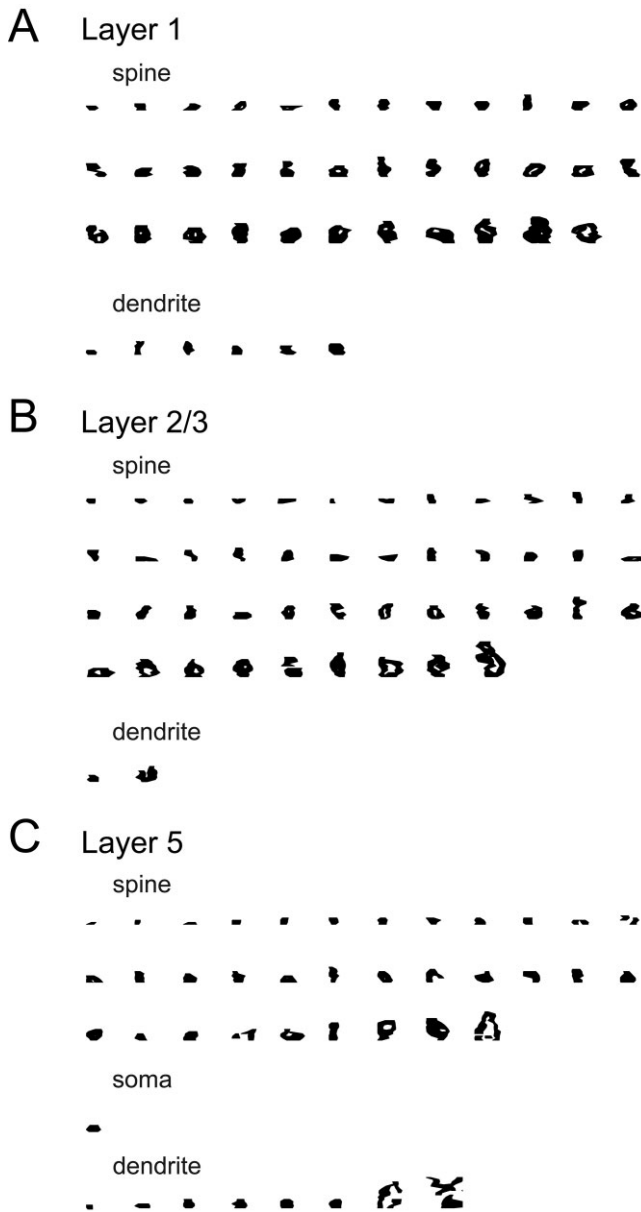


Figure 8. Two-dimensional projection of the reconstructed postsynaptic densities found on spines and dendrites postsynaptic to labeled W cell boutons. A: Layer 1. B: Layer 2/3. C: Layer 5. The densities are ordered by increasing surface area. Scale bar = 1 μm .

total number of synapses that a W axon forms with a single cortical neuron. W axons form 1.07 synapses/bouton in layer 1, 1.3 synapses/bouton in layer 2/3, and 1.26 synapses/bouton in layer 5.

DISCUSSION

In this study, we show that W-cells from the C-laminae of the dLGN form a lamina pattern of innervation of area 17 in the cat that is complementary to that of the X and Y cells. The W

axons ascend from the white matter and branch in layers 5, 3, 2, and 1, where they form asymmetric (excitatory) synapses mostly with spines. The synapses formed with spines in layer 1 are similar in area to synapses formed by X and Y axons in layer 4. The results are summarized in Figure 13. The neurons represented in Figure 13 are the major contributors of dendrite to layers 1, 2, 3, and 5 (Binzegger et al., 2004) and are, therefore, the most likely targets for the W axons, if one assumes random connectivity.

Distribution of W axons in different laminae

The putative W axons described by Ferster and LeVay (1978) were largely confined to layer 1, where the axons had prominent lateral extensions over several millimeters. Only occasionally did Ferster and LeVay (1978) observe collaterals in layers 2/3 and 5. This contrasts with the finding that layer 2/3 and also layer 5 are well labeled after injection of wheat germ agglutinin-HRP into the C laminae of the dLGN (Boyd and Matsubara, 1996; Kawano, 1998). This difference is due in part to the methods used: LeVay and Ferster could not be certain of the source of the fibers they labeled, least of all those outside layer 4. We also find that there are two classes of axon originating from the C laminae: one that arborizes extensively in layer 2/3 and then sends a thin collateral into layer 1 and another that arborizes less extensively in layer 2/3 but sends a thicker collateral to layer 1. This observation raises the question of whether both types are indeed W, insofar as the C laminae also contains some Y cells. It is unlikely that the axons we reconstructed in area 17 originated from C lamina Y cells, because these are known to project mainly to areas 18 and 19 (Hollander and Vanegas, 1977; Humphrey et al., 1985b; Leventhal, 1979). Laemle (1975) and LeVay and Ferster (1977) did not find any retrogradely labeled large cells in the C laminae after injections of HRP into area 17. The Y axons of the C lamina that project to area 17 do so almost exclusively to the upper part of layer 4 (Humphrey et al., 1985b; Leventhal, 1979) and do not, therefore, contaminate our sample. The C lamina Y axons reconstructed by Humphrey et al. (1985b) are very different from the ones shown here in that they targeted mostly upper layer 4 and the layer 3/4 border. Only one of their Y axons had a collateral extending to layer 1. The axon diameters of the C laminae axons are also much smaller than those observed for the X and Y axons that innervate layer 4.

By intracellular labeling of physiologically identified W dLGN cells, Stanford et al. (1981) showed that W cells were the class 4 neurons described by Guillery (1966). The dendritic arbors of W cells in the dLGN neurons are slightly more extensive than those of X and Y cells, and they are elongated parallel to lamina borders. The axonal input from the retina also arborizes along the plane of the lamina (Cajal, 1911 in Hayhow, 1958; Hayhow, 1958; O'Leary, 1940). These features might indicate that W dLGN cells are organized to collect input from a wide representation of visual space (Stanford et al., 1983). Retinal input represents only 2–4% of all the synapses that a W cell receives (Raczkowski et al., 1988). W cells are heterogenous with regard to the temporal and spatial summation properties of their receptive fields (Sur and Sherman, 1982) and receive different afferents depending on their sublayer of origin in the dLGN. For example, area PMLS and the superior colliculus project mainly to the deep C laminae (Graham, 1977; Harting et al., 1991; Torrealba et al., 1981;

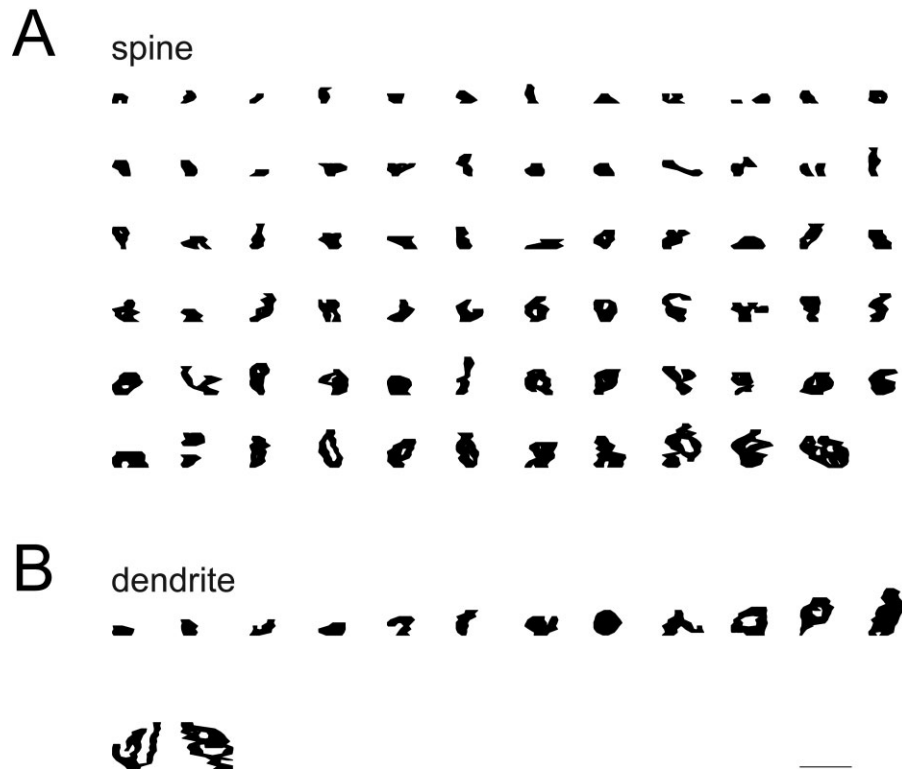


Figure 9. Two-dimensional projection of the reconstructed postsynaptic densities found in layer 4 on spines and dendrites postsynaptic to labeled X and Y cell boutons. **A:** Spines. **B:** Dendrites. The densities are ordered by increasing surface area. Scale bar = 1 μm .

Updyke, 1981). It is likely that this heterogeneity will also be reflected in the pattern of cortical innervation, as it is for the X and Y types (Ferster and LeVay, 1978; Freund et al., 1985a,b; Humphrey et al., 1985a) or magno- and parvocellular afferents in macaque monkey (Hubel and Wiesel, 1972), which also have distinctly different physiological characteristics.

Comparison with other species

The W pathway in the cat is a koniocellular pathway, which has features common to all species examined. The first common feature is that there are at least two anatomical classes of axons that target cortical layers 1 and 3. The second is that axons in layer 2/3 form patches that colocalize with cytochrome oxidase blobs. These features have been observed in koniocellular projections in the prosimian *Galago* (Diamond et al., 1985; Lachica and Casagrande, 1992), tree shrew (Usrey et al., 1992) New World squirrel and owl monkeys (Diamond et al., 1985; Fitzpatrick et al., 1983; Weber et al., 1983), and Old World macaque monkey (Casagrande et al., 2007; Hendry and Yoshioka, 1994). The third is that this pathway receives topographically organized input from the superficial layers of superior colliculus (Torrealba et al., 1981). This input is conserved in mammals with life styles as different as those of rats, cats, and primates (Harting et al., 1991). Koniocellular axons that arborize in the cytochrome blobs of primates also preferentially target spines, even though they target a larger proportion of dendritic shafts than we report here for the cat (Ding and Casagrande, 1998; Shostak et al., 2002).

Synaptic targets of W axons

Spines of pyramidal cells are the main targets of W axons. Insofar as the resident neurons of layer 1 are smooth GABAergic neurons (Gabbott and Somogyi, 1986; Li and Schwark, 1994; Prieto et al., 1994), the apical tufts of the pyramidal cells in layers 2, 3, and 5 are likely the major source of the spine targets in layer 1. In other layers, the basal dendrites of the local pyramids are likely to be the major source of spines (the apical dendrites contribute <10% of all spines (Binzegger et al., 2004). The receptive field centers of W axons can cover up to 5° in the central 10° of the visual field (Sur and Sherman, 1982), and, with their large spread of axons in layer 1, the W cells potentially provide their target pyramidal cells with an excitatory input that extends spatially beyond that provided by the X and Y cells.

PSD size and X/Y thalamic input to layer 4

The sizes of the PSDs of thalamic synapses in all the cortical layers spans an order of magnitude. Such variance is a common feature of PSD size distributions (Anderson et al., 1998; Anderson and Martin, 2002, 2005, 2006; Knott et al., 2006; Momiyama et al., 2003; Schikorski and Stevens, 1997, 1999), but the relationship between PSD size and synaptic amplitudes and dynamics has yet to be directly established. The density of AMPA receptors in the PSD has been investigated in immature Purkinje cells ($\sim 1,000/\mu\text{m}^2$; Momiyama et al., 2003; Tanaka et al., 2005) and hippocampal CA3 and CA1

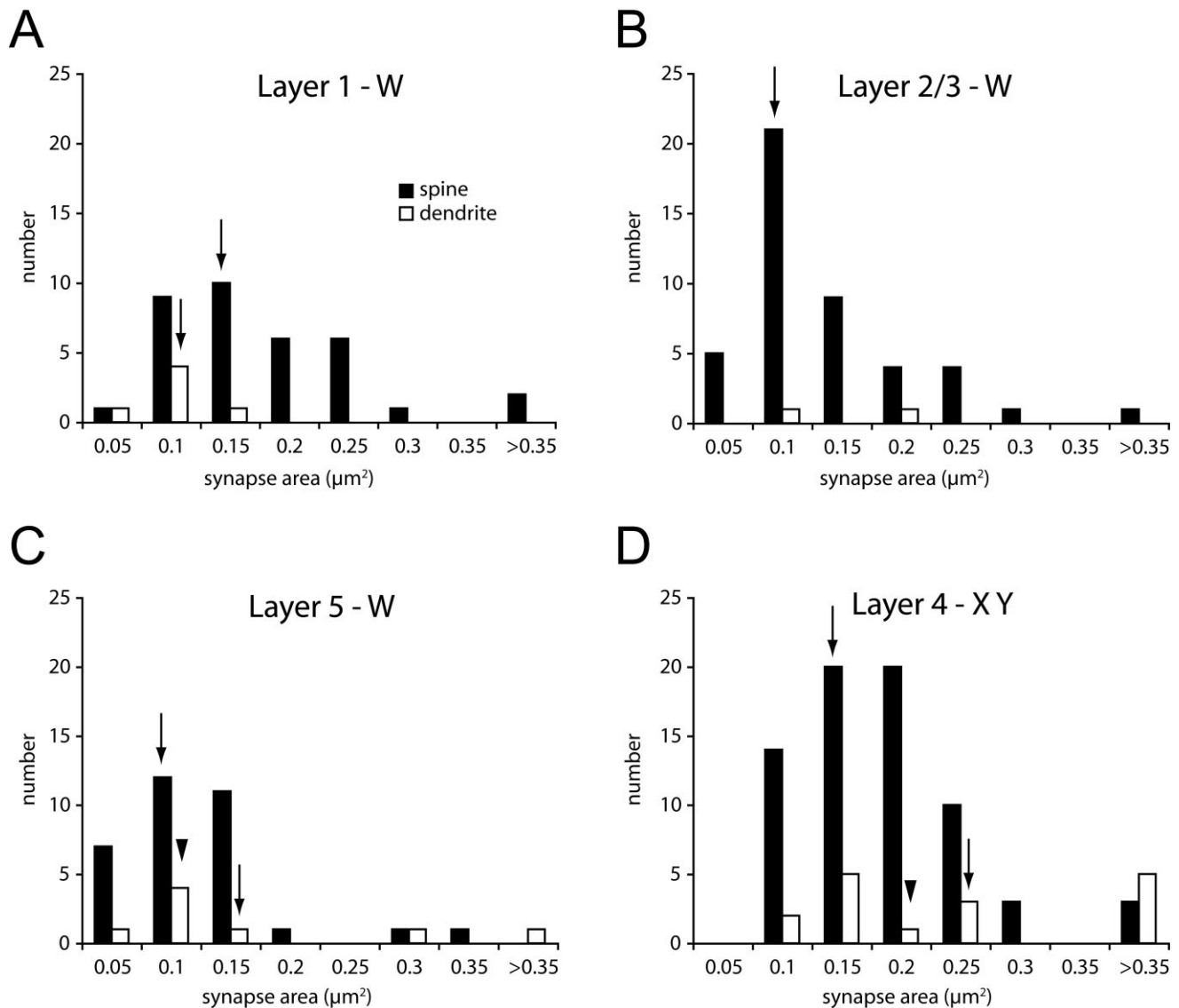


Figure 10. Histogram of the distribution of postsynaptic areas (μm^2) formed by labeled W boutons in layers 1 (A), 2/3 (B), and 5 (C) and by labeled X/Y boutons in layer 4 (D) of area 17. The mean is indicated by arrows; the median is indicated by arrowheads when it did not overlap with the mean.

spines ($525\text{--}897/\mu\text{m}^2$). If we use a receptor density of $1,000/\mu\text{m}^2$, the number of receptors in our reconstructed synapses is 162 ± 74 (mean \pm SD). In the cat, minimal stimulation of single X- and Y-type dLGN fibers evokes excitatory postsynaptic potentials (EPSPs) in spiny stellate cells in layer 4 with average amplitudes of 1.97 mV. These synapses show paired pulse depression (Stratford et al., 1996). Stratford et al. (1996) calculated that 428 ± 302 AMPA channels are required to produce their recorded EPSPs, and they concluded that their single fiber EPSPs are probably from multiple synapses. Because the release probabilities were so high, quantal analysis could not distinguish the contributions of individual release sites. We do not know how many synapses a single dLGN axon of any type forms with an individual target neuron. In a single $80\text{-}\mu\text{m}$ section, this number is usually one synapse, but

it can be as high as eight synapses (Freund et al., 1985a). Although it is probable that the PSD size correlates with amplitude, the synaptic dynamics cannot yet be inferred from the structure, so the relative contributions of the synapses of different sizes remains to be discovered.

Functional implications

The contribution of dLGN W cells to the receptive fields of cortical neurons is unknown. W cells were first described functionally for the retina and tend to have the largest receptive fields (Cleland and Levick, 1974; Stone and Hoffmann, 1972), "sluggish" responses to visual stimuli, and slow-conducting axons. W dLGN cells also have "sluggish" responses and show either linear or nonlinear spatial and tem-

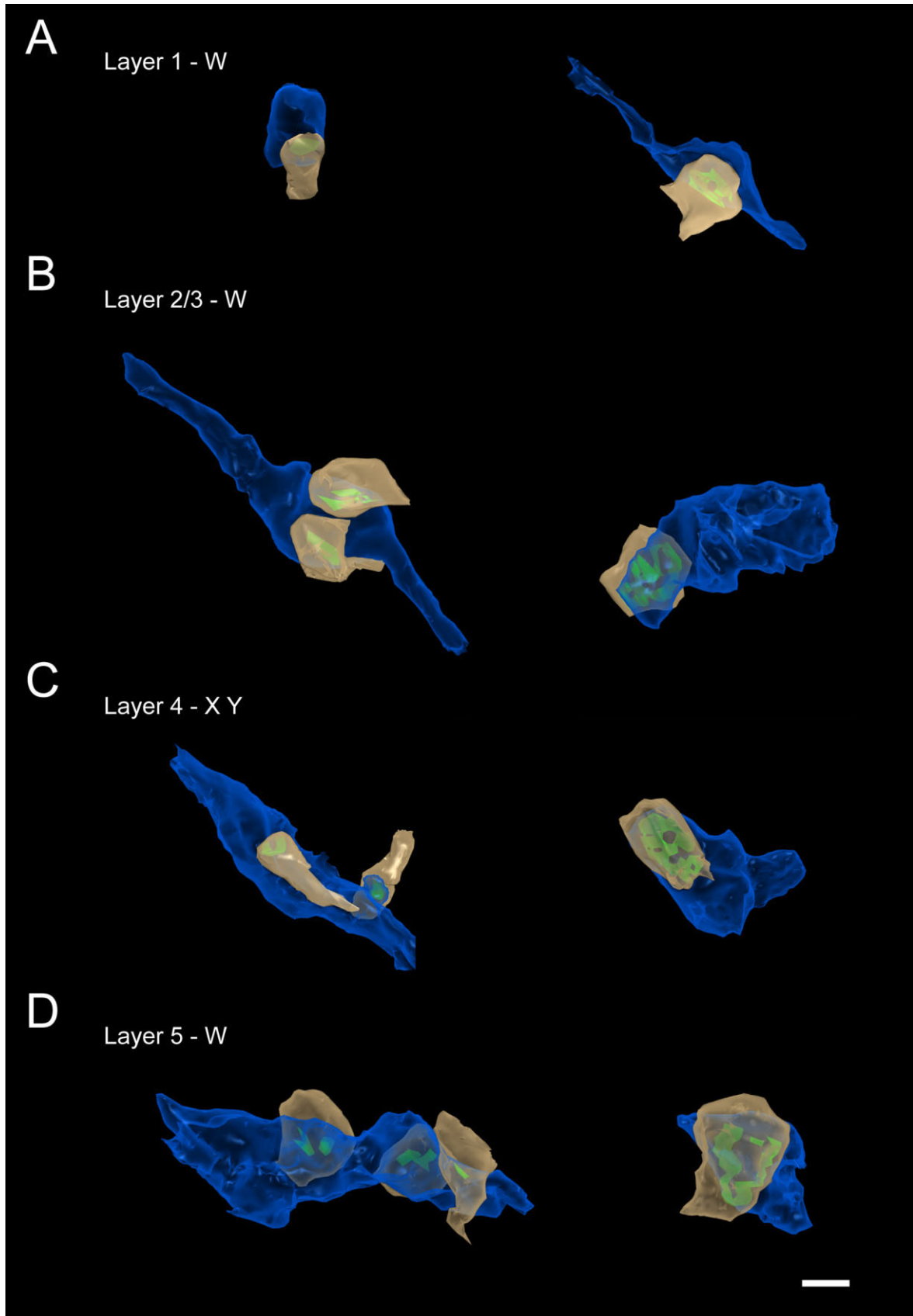


Figure 11. Three-dimensional reconstructions from serial ultrathin sections of the spines (brown) and thalamic boutons (blue) forming the smallest (left column) and largest (right column) synapse (green) in layers 1 (A), 2/3 (B), 4 (C), and 5 (D) of area 17. Scale bar = 0.5 μm .

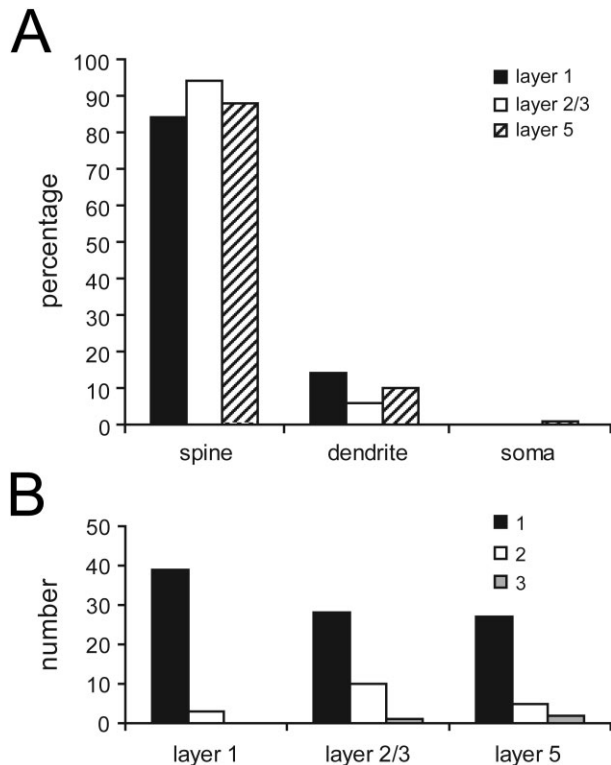


Figure 12. **A:** Histogram of the synaptic targets of labeled W cell boutons in layers 1, 2/3, and 5 of area 17. **B:** Histogram of the number of synapses formed per labeled W cell bouton in layers 1, 2/3, and 5 of area 17.

poral summation (Cleland et al., 1975; Stanford et al., 1981; Sur and Sherman, 1982). Thus, the relatively slow time course of response of the W pathway, combined with its input to distal parts of the dendritic tree, will temporally smear the response relative to that of the X and Y pathways. This may allow the W pathway to act as a short-term memory store, which would be useful for short-duration changes in gain or sensitivity.

Nothing is known about the efficacy of the synapses formed by W axons. Our ultrastructural data suggest that local EPSPs evoked by layer 1 W boutons should be similar to those evoked by X and Y axons in layer 4, insofar as the synapse areas of W axons formed with spines in layer 1 are not significantly different from synapses formed by X and Y boutons in layer 4. In addition, there may be a postsynaptic amplification of the effects of W-synapses in layer 1, because the apical tuft of layer 5 pyramidal neurons contain an active calcium conductance. In rats, stimulation of layer 1 leads to minimal evoked EPSPs of large amplitude (2.11–7.17 mV; Larkum and Zhu, 2002) that can evoke burst firing, and it is possible that the W axons contribute to this activation in the cat. In addition, it has been proposed that near-synchronous input to both apical tufts and basal dendrites can facilitate the generation of bursts by layer 5 pyramidal neurons (Larkum et al., 1999). The distribution of the W axon in the cortex provides one possibility of implementing such a mechanism. Physiological evidence from Llinas et al. (2002) indicates that, compared with individual activation of the ventrobasal thalamic nucleus, si-

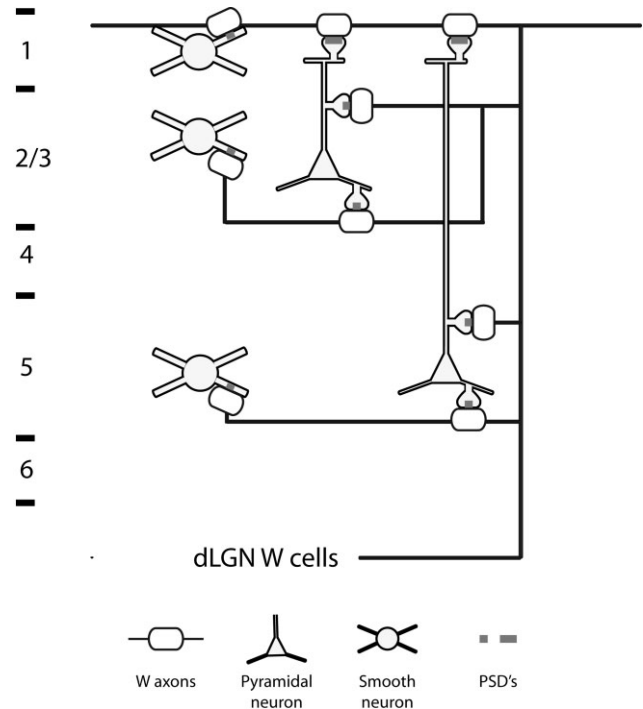


Figure 13. Summary diagram of the projection of W axons to area 17, which innervates layers 1, 2, 3, and 5. Although not directly demonstrated, the pyramidal neurons of layers 2, 3, and 5 are the probable targets, insofar as they contribute the most dendrites to the layers innervated by W axons. More selective connections could not be demonstrated.

multaneous activation of this nucleus and either the centrolateral nucleus or layer 1, produces supralinear responses of layer 5 neurons in mouse barrel cortex. As in the rodent, the cat's W projection to layer 1, with its large synapses, might have an instructor role in changing the firing mode of layer 5 pyramidal neurons to burst. The layer 5 pyramidal neurons that project to the superior colliculus in the cat (Hollander, 1974) have an apical dendrite that forms a large tuft in layer 1 (Hubener et al., 1990) and are potential targets of the W relay neurons from the C2 and C3 lamina. The W cells from the most ventral C laminae are the only relay neurons that receive input from the superior colliculus, which controls saccadic eye movements. Such a combination of bursting activity during saccadic eye movements is observed in monkey V1 neurons, which tend to fire in bursts when microsaccades move the receptive field of the neuron across a stimulus of the preferred orientation (Martinez-Conde et al., 2000, 2002). Even though the cat does not produce microsaccades (Winterson and Robinson, 1975), it does have saccadic and other eye movement where such modulation can take place. Thus, the W projection, so long a minor footnote in the history of thalamic relay cells, may yet prove to be relevant for the generation of visually guided behavior.

ACKNOWLEDGMENTS

We thank Rita Bopp and German Koestinger for their expert technical assistance.

LITERATURE CITED

- Abramson BP, Chalupa LM. 1985. The laminar distribution of cortical connections with the tecto- and cortico-recipient zones in the cat's lateral posterior nucleus. *Neuroscience* 15:81-95.
- Ahmed B, Anderson JC, Douglas RJ, Martin KA, Nelson JC. 1994. Poly-neuronal innervation of spiny stellate neurons in cat visual cortex. *J Comp Neurol* 341:39-49.
- Ahmed B, Anderson JC, Martin KA, Nelson JC. 1997. Map of the synapses onto layer 4 basket cells of the primary visual cortex of the cat. *J Comp Neurol* 380:230-242.
- Anderson JC, Martin KA. 2002. Connection from cortical area V2 to MT in macaque monkey. *J Comp Neurol* 443:56-70.
- Anderson JC, Martin KA. 2005. Connection from cortical area V2 to V3 A in macaque monkey. *J Comp Neurol* 488:320-330.
- Anderson JC, Martin KA. 2006. Synaptic connection from cortical area V4 to V2 in macaque monkey. *J Comp Neurol* 495:709-721.
- Anderson JC, Binzegger T, Martin KA, Rockland KS. 1998. The connection from cortical area V1 to V5: a light and electron microscopic study. *J Neurosci* 18:10525-10540.
- Beaulieu C, Colonnier M. 1985. A laminar analysis of the number of round-asymmetrical and flat-symmetrical synapses on spines, dendritic trunks, and cell bodies in area 17 of the cat. *J Comp Neurol* 231:180-189.
- Binzegger T, Douglas RJ, Martin KA. 2004. A quantitative map of the circuit of cat primary visual cortex. *J Neurosci* 24:8441-8453.
- Boyd JD, Matsubara JA. 1996. Laminar and columnar patterns of geniculocortical projections in the cat: relationship to cytochrome oxidase. *J Comp Neurol* 365:659-682.
- Casagrande VA, Yazar F, Jones KD, Ding Y. 2007. The morphology of the koniocellular pathway in the macaque monkey. *Cereb Cortex* 17:2334-2345.
- Clarke RH, Henderson EE. 1914. Atlas of photographs of sections of the frozen cranium and brain of the cat. II. Frontal sections. *J Psychiatr Neurol* 21:273-277.
- Cleland BG, Levick WR. 1974. Brisk and sluggish concentrically organized ganglion cells in the cat's retina. *J Physiol* 240:421-456.
- Cleland BG, Morstyn R, Wagner HG, Levick WR. 1975. Long-latency retinal input to lateral geniculate neurones of the cat. *Brain Res* 91:306-310.
- Diamond IT, Conley M, Itoh K, Fitzpatrick D. 1985. Laminar organization of geniculocortical projections in *Galago senegalensis* and *Aotus trivirgatus*. *J Comp Neurol* 242:584-610.
- Ding Y, Casagrande VA. 1998. Synaptic and neurochemical characterization of parallel pathways to the cytochrome oxidase blobs of primate visual cortex. *J Comp Neurol* 391:429-443.
- Ferster D, LeVay S. 1978. The axonal arborizations of lateral geniculate neurons in the striate cortex of the cat. *J Comp Neurol* 182:923-944.
- Fiala JC. 2005. Reconstruct: a free editor for serial section microscopy. *J Microsc* 218:52-61.
- Fitzpatrick D, Itoh K, Diamond IT. 1983. The laminar organization of the lateral geniculate body and the striate cortex in the squirrel monkey (*Saimiri sciureus*). *J Neurosci* 3:673-702.
- Freund TF, Martin KA, Somogyi P, Whitteridge D. 1985a. Innervation of cat visual areas 17 and 18 by physiologically identified X- and Y-type thalamic afferents. II. Identification of postsynaptic targets by GABA immunocytochemistry and Golgi impregnation. *J Comp Neurol* 242:275-291.
- Freund TF, Martin KA, Whitteridge D. 1985b. Innervation of cat visual areas 17 and 18 by physiologically identified X- and Y-type thalamic afferents. I. Arborization patterns and quantitative distribution of postsynaptic elements. *J Comp Neurol* 242:263-274.
- Gabbott PL, Somogyi P. 1986. Quantitative distribution of GABA-immunoreactive neurons in the visual cortex (area 17) of the cat. *Exp Brain Res* 61:323-331.
- Geisert EE Jr. 1980. Cortical projections of the lateral geniculate nucleus in the cat. *J Comp Neurol* 190:793-812.
- Gilbert CD, Wiesel TN. 1979. Morphology and intracortical projections of functionally characterized neurones in the cat visual cortex. *Nature* 280:120-125.
- Gilbert CD, Wiesel TN. 1983. Clustered intrinsic connections in cat visual cortex. *J Neurosci* 3:1116-1133.
- Graham J. 1977. An autoradiographic study of the efferent connections of the superior colliculus in the cat. *J Comp Neurol* 173:629-654.
- Guillery RW. 1966. A study of Golgi preparations from the dorsal lateral geniculate nucleus of the adult cat. *J Comp Neurol* 128:21-50.
- Guillery RW. 1970. The laminar distribution of retinal fibers in the dorsal lateral geniculate nucleus of the cat: a new interpretation. *J Comp Neurol* 138:339-366.
- Harting JK, Huerta MF, Hashikawa T, van Lieshout DP. 1991. Projection of the mammalian superior colliculus upon the dorsal lateral geniculate nucleus: organization of tectogeniculate pathways in nineteen species. *J Comp Neurol* 304:275-306.
- Hayhow WR. 1958. The cytoarchitecture of the lateral geniculate body in the cat in relation to the distribution of crossed and uncrossed optic fibers. *J Comp Neurol* 110:1-63.
- Hendry SH, Yoshioka T. 1994. A neurochemically distinct third channel in the macaque dorsal lateral geniculate nucleus. *Science* 264:575-577.
- Henry GH, Salin PA, Bullier J. 1991. Projections from areas 18 and 19 to cat striate cortex: divergence and laminar specificity. *Eur J Neurosci* 3:186-200.
- Hickey TL, Guillery RW. 1974. An autoradiographic study of retinogeniculate pathways in the cat and the fox. *J Comp Neurol* 156:239-253.
- Hollander H. 1974. On the origin of the corticotectal projections in the cat. *Exp Brain Res* 21:433-439.
- Hollander H, Vanegas H. 1977. The projection from the lateral geniculate nucleus onto the visual cortex in the cat. A quantitative study with horseradish-peroxidase. *J Comp Neurol* 173:519-536.
- Hubel DH, Wiesel TN. 1972. Laminar and columnar distribution of geniculocortical fibers in the macaque monkey. *J Comp Neurol* 146:421-450.
- Hubener M, Schwarz C, Bolz J. 1990. Morphological types of projection neurons in layer 5 of cat visual cortex. *J Comp Neurol* 301:655-674.
- Humphrey AL, Sur M, Uhlrich DJ, Sherman SM. 1985a. Projection patterns of individual X- and Y-cell axons from the lateral geniculate nucleus to cortical area 17 in the cat. *J Comp Neurol* 233:159-189.
- Humphrey AL, Sur M, Uhlrich DJ, Sherman SM. 1985b. Termination patterns of individual X- and Y-cell axons in the visual cortex of the cat: projections to area 18, to the 17/18 border region, and to both areas 17 and 18. *J Comp Neurol* 233:190-212.
- Kawano J. 1998. Cortical projections of the parvocellular laminae C of the dorsal lateral geniculate nucleus in the cat: an anterograde wheat germ agglutinin conjugated to horseradish peroxidase study. *J Comp Neurol* 392:439-457.
- Kisvarday ZF, Martin KA, Whitteridge D, Somogyi P. 1985. Synaptic connections of intracellularly filled clutch cells: a type of small basket cell in the visual cortex of the cat. *J Comp Neurol* 241:111-137.
- Knott GW, Holtmaat A, Wilbrecht L, Welker E, Svoboda K. 2006. Spine growth precedes synapse formation in the adult neocortex in vivo. *Nat Neurosci* 9:1117-1124.
- Lachica EA, Casagrande VA. 1992. Direct W-like geniculate projections to the cytochrome oxidase (CO) blobs in primate visual cortex: axon morphology. *J Comp Neurol* 319:141-158.
- Laemle LK. 1975. Cell populations of the lateral geniculate nucleus of the cat as determined with horseradish peroxidase. *Brain Res* 100:650-656.
- Larkum ME, Zhu JJ. 2002. Signaling of layer 1 and whisker-evoked Ca²⁺ and Na⁺ action potentials in distal and terminal dendrites of rat neocortical pyramidal neurons in vitro and in vivo. *J Neurosci* 22:6991-7005.
- Larkum ME, Zhu JJ, Sakmann B. 1999. A new cellular mechanism for coupling inputs arriving at different cortical layers. *Nature* 398:338-341.
- LeVay S, Ferster D. 1977. Relay cell classes in the lateral geniculate nucleus of the cat and the effects of visual deprivation. *J Comp Neurol* 172:563-584.
- LeVay S, Gilbert CD. 1976. Laminar patterns of geniculocortical projection in the cat. *Brain Res* 113:1-19.
- LeVay S, Sherk H. 1981. The visual claustrum of the cat. I. Structure and connections. *J Neurosci* 1:956-980.
- Leventhal AG. 1979. Evidence that the different classes of relay cells of the cat's lateral geniculate nucleus terminate in different layers of the striate cortex. *Exp Brain Res* 37:349-372.
- Li J, Schwark HD. 1994. Distribution and proportions of GABA-immunoreactive neurons in cat primary somatosensory cortex. *J Comp Neurol* 343:353-361.
- Llinas RR, Leznik E, Urbano FJ. 2002. Temporal binding via cortical coincidence detection of specific and nonspecific thalamocortical in-

- puts: a voltage-dependent dye-imaging study in mouse brain slices. *Proc Natl Acad Sci U S A* 99:449–454.
- Martinez-Conde S, Macknik SL, Hubel DH. 2000. Microsaccadic eye movements and firing of single cells in the striate cortex of macaque monkeys. *Nat Neurosci* 3:251–258.
- Martinez-Conde S, Macknik SL, Hubel DH. 2002. The function of bursts of spikes during visual fixation in the awake primate lateral geniculate nucleus and primary visual cortex. *Proc Natl Acad Sci U S A* 99:13920–13925.
- Momiyama A, Silver RA, Hausser M, Notomi T, Wu Y, Shigemoto R, Cull-Candy SG. 2003. The density of AMPA receptors activated by a transmitter quantum at the climbing fibre-Purkinje cell synapse in immature rats. *J Physiol* 549:75–92.
- O'Leary JL. 1940. A structural analysis of the lateral geniculate nucleus of the cat. *J Comp Neurol* 73:405–430.
- Peters A, Saint Marie RL. 1984. Smooth and sparsely spinous non-pyramidal cells forming local axonal plexuses. In: Jones EG, Peters A, editors. *Cerebral cortex*. New York: Plenum, p 419–445.
- Peters A, Palay SL, Webster F. 1991. *The fine structure of the nervous system: neurons and their supporting cells*. Oxford: Oxford University Press.
- Prieto JJ, Peterson BA, Winer JA. 1994. Morphology and spatial distribution of GABAergic neurons in cat primary auditory cortex (AI). *J Comp Neurol* 344:349–382.
- Raczkowski D, Rosenquist AC. 1980. Connections of the parvocellular C laminae of the dorsal lateral geniculate nucleus with the visual cortex in the cat. *Brain Res* 199:447–451.
- Raczkowski D, Hamos JE, Sherman SM. 1988. Synaptic circuitry of physiologically identified W-cells in the cat's dorsal lateral geniculate nucleus. *J Neurosci* 8:31–48.
- Sanderson KJ. 1971. The projection of the visual field to the lateral geniculate and medial interlaminar nuclei in the cat. *J Comp Neurol* 143:101–108.
- Schikorski T, Stevens CF. 1997. Quantitative ultrastructural analysis of hippocampal excitatory synapses. *J Neurosci* 17:5858–5867.
- Schikorski T, Stevens CF. 1999. Quantitative fine-structural analysis of olfactory cortical synapses. *Proc Natl Acad Sci U S A* 96:4107–4112.
- Shatz CJ. 1977. Anatomy of interhemispheric connections in the visual system of Boston Siamese and ordinary cats. *J Comp Neurol* 173:497–518.
- Shostak Y, Ding Y, Mavity-Hudson J, Casagrande VA. 2002. Cortical synaptic arrangements of the third visual pathway in three primate species: *Macaca mulatta*, *Saimiri sciureus*, and *Aotus trivirgatus*. *J Neurosci* 22:2885–2893.
- Somogyi P, Kisvarday ZF, Martin KA, Whitteridge D. 1983. Synaptic connections of morphologically identified and physiologically characterized large basket cells in the striate cortex of cat. *Neuroscience* 10:261–294.
- Stanford LR, Friedlander MJ, Sherman SM. 1981. Morphology of physiologically identified W-cells in the C laminae of the cat's lateral geniculate nucleus. *J Neurosci* 1:578–584.
- Stanford LR, Friedlander MJ, Sherman SM. 1983. Morphological and physiological properties of geniculate W-cells of the cat: a comparison with X- and Y-cells. *J Neurophysiol* 50:582–608.
- Sterio DC. 1984. The unbiased estimation of number and sizes of arbitrary particles using the disector. *J Microsc* 134:127–136.
- Stone J, Hoffmann KP. 1972. Very slow-conducting ganglion cells in the cat's retina: a major, new functional type? *Brain Res* 43:610–616.
- Stratford KJ, Tarczy-Hornoch K, Martin KA, Bannister NJ, Jack JJ. 1996. Excitatory synaptic inputs to spiny stellate cells in cat visual cortex. *Nature* 382:258–261.
- Sur M, Sherman SM. 1982. Linear and nonlinear W-cells in C-laminae of the cat's lateral geniculate nucleus. *J Neurophysiol* 47:869–884.
- Symonds LL, Rosenquist AC, Edwards SB, Palmer LA. 1981. Projections of the pulvinar-lateral posterior complex to visual cortical areas in the cat. *Neuroscience* 6:1995–2020.
- Tanaka J, Matsuzaki M, Tarusawa E, Momiyama A, Molnar E, Kasai H, Shigemoto R. 2005. Number and density of AMPA receptors in single synapses in immature cerebellum. *J Neurosci* 25:799–807.
- Torrealba F, Partlow GD, Guillery RW. 1981. Organization of the projection from the superior colliculus to the dorsal lateral geniculate nucleus of the cat. *Neuroscience* 6:1341–1360.
- Updyke BV. 1981. Projections from visual areas of the middle suprasylvian sulcus onto the lateral posterior complex and adjacent thalamic nuclei in cat. *J Comp Neurol* 201:477–506.
- Usrey WM, Muly EC, Fitzpatrick D. 1992. Lateral geniculate projections to the superficial layers of visual cortex in the tree shrew. *J Comp Neurol* 319:159–171.
- Weber JT, Huerta MF, Kaas JH, Harting JK. 1983. The projections of the lateral geniculate nucleus of the squirrel monkey: studies of the interlaminar zones and the S layers. *J Comp Neurol* 213:135–145.
- Winterson BJ, Robinson DA. 1975. Fixation by the alert but solitary cat. *Vis Res* 15:1349–1352.